Article:
El-Asrag, ME, Sergouniotis, PI, McKibbin, M et al. (16 more authors) (2015) Biallelic Mutations in the Autophagy Regulator DRAM2 Cause Retinal Dystrophy with Early Macular Involvement. American Journal of Human Genetics, 96 (6). 948 - 954. ISSN 0002-9297

https://doi.org/10.1016/j.ajhg.2015.04.006

Biallelic mutations in the autophagy regulator *DRAM2* cause retinal dystrophy with early macular involvement

Mohammed E. El-Asrag[1,2,13], Panagiotis I. Sergouniotis[3,4,13], Martin McKibbin[5], Vincent Plagnol[6], Eamonn Sheridan[7], Naushin Waseem[3], Zakia Abdelhamed[1], Declan McKeefry[8], Kristof Van Schil[9], James A. Poulter[1], UK Inherited Retinal Disease Consortium, Colin A. Johnson[1], Ian M. Carr[1], Bart P. Leroy[9,10,11], Elfride De Baere[9], Chris F. Inglehearn[1], Andrew R. Webster[3,12], Carmel Toomes[1]**, Manir Ali[1]*

[1] Section of Ophthalmology and Neuroscience, Leeds Institute of Biomedical and Clinical Sciences, University of Leeds, Leeds LS9 7TF, UK.

[2] Department of Zoology, Faculty of Science, Benha University, 13511 Benha, Egypt.

[3] UCL Institute of Ophthalmology, University College London, London EC1V 9EL, UK.

[4] Institute of Human Development, Faculty of Medical and Human Sciences, University of Manchester, Manchester M13 9WL, UK.

[5] Department of Ophthalmology, St. James's University Hospital, Leeds LS9 7TF, UK.

[6] UCL Genetics Institute, University College London, London WC1E 6BT, UK.

[7] Yorkshire Regional Genetics Service, St. James's University Hospital, Leeds LS9 7TF, UK.

[8] Bradford School of Optometry and Visual Science, University of Bradford, Bradford BD7 1DP, UK.

[9] Center for Medical Genetics, Ghent University Hospital, 9000 Ghent, Belgium.

[10] Department of Ophthalmology, Ghent University Hospital, 9000 Ghent, Belgium.

[11] Division of Ophthalmology, The Children's Hospital of Philadelphia, Philadelphia 19104, USA.

[12] Moorfields Eye Hospital, London EC1V 2PD, UK.

[13] These authors contributed equally to this work.

Correspondence:

*medma@leeds.ac.uk

**c.toomes@leeds.ac.uk

Short title: *DRAM2* mutations cause retinal dystrophy.

Abstract

Retinal dystrophies are an overlapping group of genetically heterogeneous conditions resulting from mutations in over 250 genes. Here we describe five families affected by an adult-onset retinal dystrophy with early macular involvement and associated central visual loss in the third/fourth decade of life. Affected individuals were found to harbor disease causing variants in *DRAM2* (DNA-damage regulated autophagy modulator protein 2). Homozygosity mapping and exome sequencing in a large, consanguineous British family of Pakistani origin revealed a homozygous frameshift variant (c.140delG, p.Gly47Valfs*3) in nine affected family members. Sanger sequencing of *DRAM2* in 322 unrelated probands with retinal dystrophy revealed one European subject with compound heterozygous *DRAM2* changes (c.494G>A, p.Trp165* and c.131G>A, p.Ser44Asn). Inspection of previously generated exome sequencing data in unsolved retinal dystrophy cases identified a homozygous variant in an individual of Indian origin (c.64_66del, p.Ala22del). Independently, a gene-based case-control association study was conducted using an exome sequencing dataset of 18 phenotypically similar cases and 1,917 controls. Using a recessive model and a binomial test for rare, presumed biallelic, variants, *DRAM2* was found to be the most statistically-enriched gene; one subject was a homozygote (c.362A>T, p.His121Leu) and another a compound heterozygote (c.79T>C, p.Tyr27His and c.217_225del, p.Val73_Tyr75del). *DRAM2* encodes a transmembrane lysosomal protein thought to play a role in the initiation of autophagy. Immunohistochemical analysis showed DRAM2 localization to photoreceptor inner segments and to the apical surface of retinal pigment epithelial cells where it may be involved in the process of photoreceptor renewal and recycling to preserve visual function.

Retinal dystrophies are a clinically and genetically heterogeneous group of disorders characterized by progressive photoreceptor degeneration.[1] The pattern of visual loss and retinal appearance varies and is related to the degree to which cone and rod photoreceptors are affected. In subjects with retinitis pigmentosa (RP), for example, the rods are affected more severely and earlier than the cones, and the presenting symptoms are typically night blindness and/or visual field loss. Disorders in which the cones are more severely affected than the rods include macular dystrophies (MD; localized loss of central/macular cones as a primary or secondary event) and cone-rod dystrophies (CRD; central and peripheral cone involvement). MD and CRD show clinical overlap and loss of central vision is often the common presenting symptom. Frequently, subjects with CRD also report light sensitivity, a symptom which can suggest generalized cone system dysfunction. Assigning a disease category can sometimes be challenging with confounding factors being inter- and intra-familial phenotypic variability and the presence of age-dependent phenotypic transitions. RP, MD and CRD can be transmitted in a dominant, recessive or X-linked manner and, to date, variants in 70, 14 and 30 genes respectively have been shown to give rise to these conditions (RetNet, accessed February 2015).

The initial aim of this study was to identify the genetic basis of an adult-onset retinal dystrophy with early macular involvement (Figure 1) in a consanguineous Pakistani family with multiple affected members living in the UK (family ES1; Figure 2). Affected individuals became symptomatic early in the third decade, describing increasing difficulty with close visual tasks. Neither light sensitivity nor night blindness were significant early symptoms. There was progressive loss of visual acuity in all symptomatic individuals; light sensitivity and difficulty seeing in dim illumination were inconsistent features of advanced disease. Fundus examination revealed maculopathy in all symptomatic individuals tested, with peripheral retinal degeneration being a frequent finding in older subjects. Notably, optical coherence tomography (OCT) imaging in the pre-symptomatic second decade (subject IV.9, family ES1; Figure 2) suggested early central photoreceptor cell loss.

This study was approved by the Leeds East (Project number 03/362), Moorfields Eye Hospital and Ghent University Hospital (PA2015/012) Research Ethics Committees and adhered to the tenets of the Declaration of Helsinki. Individuals participated in

the study following their informed consent. Peripheral blood was collected from affected individuals, parents and unaffected relatives where these were available. Genomic DNA was extracted from blood leukocytes according to standard procedures.

Homozygosity mapping was performed using Affymetrix 250K single nucleotide polymorphism (SNP) arrays on genomic DNA from seven affected individuals from family ES1. Data were analysed with the AgileMultiIdeogram software. Two homozygous regions were shared among all seven affected individuals: a 10.1Mb interval on chromosome 1 (between rs6677953 and rs814987; containing 160 genes) and a 2.9Mb region on chromosome 7 (between rs17140297 and rs12706292; containing 5 genes) (Figure S1). Given the absence of genes previously reported to be associated with retinal dystrophy within these intervals, a whole exome sequencing (WES) strategy was utilized to identify the molecular pathology in the family. DNA from one affected family member (subject IV.6, family ES1; Figure 2) was analysed using a HiSeq2000 system (Illumina). After aligning the sequencing data output against the reference genome (hg19/GRCh37) as well as variant calling and filtration steps, a list of 33 homozygous variants was generated (Table S1). Only one of these sequence alterations mapped within the shared regions of homozygosity identified in family ES1. This was a homozygous single-base deletion in *DRAM2* (DNA-damage regulated autophagy modulator protein 2 [MIM 613360], NM_178454.4), that creates a frameshift and is predicted to lead to premature truncation of the protein (c.140delG, p.Gly47Valfs*3). Segregation of this variant with the disease in the family (Figure 2) was confirmed by Sanger sequencing of *DRAM2* exon 4 (Figure 3A; primer pairs are shown in Table S2). This change was excluded from 159 ethnically matched control individuals and was not present in the dbSNP and EVS databases. It was found once in heterozygous state in WES data from 61,486 unrelated individuals sequenced as part of various disease-specific and population genetic studies (accessed via. the Exome Aggregation Consortium [ExAC] browser, version 0.2). Notably, no homozygous presumed loss-of-function variant in *DRAM2* was present in the ExAC dataset. A maximum two point LOD score of 2.4 was obtained between c.140delG and the disease in nine genotyped family members using Superlink.[2] For this analysis the c.140delG change was treated as a genetic marker with a MAF of 0.01%, and the

disease was assumed to segregate in the family in a recessive fashion with full penetrance.

In an attempt to identify further families with *DRAM2*-associated retinopathy, the seven coding *DRAM2* exons and flanking splice sites, were PCR amplified and Sanger sequenced in 74 individuals diagnosed with RP, 154 with CRD or MD and 94 with infantile-onset retinal dystrophy (Leber Congenital Amaurosis) (primer pairs are shown in Table S2). This screen identified an isolated female case (subject 1325) of European ancestry in the CRD/MD panel that was compound heterozygous for a nonsense variant in exon 6 (c.494G>A, p.Trp165*) and a missense change in exon 3 (c.131G>A, p.Ser44Asn). The latter affects a serine residue that is conserved from human to nematodes (Figures 3 and S2). This missense change was predicted to be pathogenic by a number of bioinformatics prediction tools (Table S3) and was not present in dbSNP, EVS or ExAC databases. The c.494G>A change is an annotated variant in dbSNP (rs201422368) with a MAF of 0.008% (1/13,003) in EVS and 0.003% (3/118,572) in ExAC; it is only reported in heterozygous state in these databases. Subject 1325 experienced blurred vision at age 29 and was soon after found to have maculopathy on fundus examination. At age 35, she also complained of night vision problems and sensitivity to light; fundus examination revealed mild peripheral retinal degeneration in addition to the maculopathy. At the age of 47, she had acuity of 1.0 logMAR in each eye and electrophysiology revealed severely attenuated or absent full-field electroretinograms (ERGs) and pattern ERGs (Figure S3).

Meanwhile, interrogation of previously generated WES data from unsolved cases with retinal dystrophy lead to the identification of a homozygous variant in exon 3 of *DRAM2* (c.64_66del, p.Ala22del) in a subject of Indian origin. This change, which removes an alanine residue from the first transmembrane domain of the molecule, was predicted to be pathogenic using bioinformatics prediction tools (Table S3) and was absent in dbSNP, EVS and ExAC databases. The variant was confirmed by Sanger sequencing (Figure 3) and segregated in family BL1 with the disease as expected in a recessive manner (Figure 2). The affected subject, a lady in her early forties, has maculopathy with a normal full-field ERG indicating absence of a generalised retinal dysfunction. The individual also suffers from iron-deficiency

anaemia, which may have been brought on by a vegetarian diet or may be the result of a genetic factor due to parental consanguinity.

Independently, in a study designed to identify novel genes associated with retinal disease, 28 families from the inherited retinal disease clinics at Moorfields Eye Hospital, London were ascertained. Details on this cohort have been previously reported.[3] The main inclusion criteria included a CRD or MD phenotype and an absence of retinal imaging findings suggestive of *ABCA4*-retinopathy. Genomic DNA from the probands was analyzed by WES and variant filtering was performed as previously described.[3] The molecular diagnosis was identified in 10 of 28 families.[3] On the 18 unsolved cases, a gene based case-control association analysis was performed utilising WES data generated by a consortium of UK based researchers ("UCL-exomes", Table S4). Aiming to minimize bias,[4] UCL-exomes controls were initially split into two sets. The first set of 500 randomly selected samples was used in conjunction with EVS to determine variant frequency for inclusion in case control tests. In that context, "rare" variants are variants with MAF<0.5% in EVS and no more than 2 occurrences in this first set of 500 UCL-exomes control samples. The second set of 1,917 unrelated UCL-exomes controls was used to directly compute gene based association p-values, using a recessive disease mode, *i.e*. samples were labeled as potential carriers only if they carried at least two rare (using the definition stated above) and potentially functional (presumed loss-of-function, non-synonymous or splice site altering) variants. A binomial test was used for excess of such potential biallelic variants in the 18 cases compared to the 1,917 controls (Table S4).

The most significant gene-based p-value was obtained for *DRAM2* (Table S4). Two of the 18 cases were found to harbor likely disease-associated variants in this gene. A 37-year-old female proband (family gc17004, Figure 2) of European ancestry was a compound heterozygote for a missense variant (c.79T>C, p.Tyr27His) and an in-frame deletion (c.217_225del, p.Val73_Tyr75del). Furthermore, a 47-year-old male proband of South Asian origin (family gc4728, Figure 2; parents not knowingly related) was homozygous for a missense change (c.362A>T, p.His121Leu). None of these three changes which are reported to be pathogenic by a number of prediction tools (Table S3) exist in dbSNP, EVS or ExAC. Both missense variants, p.Tyr27His

and p.His121Leu, affect a tyrosine and histidine residue respectively that are evolutionarily conserved from human to nematodes (Figure S2).. All changes were confirmed by Sanger sequencing (Figure 3) and segregated with the disease phenotype in the family as expected for a recessive condition (Figure 2).

Both probands presented with central visual loss (at age 29 for the proband of family gc17004 and at age 37 for the proband of family gc4728). At presentation, fundus examination and retinal imaging revealed macular photoreceptor loss with an apparently normal peripheral retina. These observations were consistent with electrophysiological findings. Notably, 8 years after presentation, the central areas of atrophy have expanded and peripheral changes were observed. Electrodiagnostic testing was repeated and revealed more widespread retinal dysfunction in both cases. The phenotype was notably similar to the affected members of families ES1, BL1 and subject 1325 described above.

Given that affected members of family ES1 are homozygous for a *DRAM2* variant that is likely to lead to either nonsense mediated decay of the encoded mRNA, or to a truncated protein of only 47 amino acids, the molecular pathology of the disease is likely to be loss of DRAM2 function. This speculation is further supported by the biallelic state and predicted severity of the additional six likely disease-causing variants identified as well as by the similar phenotype in all five families.

DRAM2, also known as TMEM77 (transmembrane protein 77), encodes a 266 amino acid protein containing six putative transmembrane domains (Figure 3B). Previous overexpression studies in HEK293 cells localised it to lysosomal membranes[5,6] where it initiates the conversion of endogenous LC3-I (microtubule-associated protein light chain 3) to the general autophagosome marker protein, LC3-II (LC3-1/phosphatidylethanolamine conjugate). This suggests that DRAM2 induces the autophagy process.[5] Autophagy is a natural cell survival mechanism triggered in response to stress stimuli such as nutrient starvation or the accumulation of damaged organelles. It is responsible for degrading and recycling cytoplasmic proteins and lipids as well as organelles within the cell.[7] This usually begins with isolation of the macromolecules and organelles within the cytoplasm into single membrane vesicles, which fuse together to produce an autophagosome. These

autophagosomes subsequently fuse with lysosomes containing acid hydrolases and form a double-membrane autolysosome.[8,9] Although the aim of autophagy is to relieve cellular stress, its excessive induction can in some cases lead to apoptosis rather than protection from cell death.[10]

There is also some evidence to suggest that DRAM2 may have tumour suppressor capability. DRAM2 transcript and protein expression are reduced in ovarian tumours compared to normal matched tissues.[5] Also, siRNA knockdown of endogenous DRAM2 results in reduced conversion to LC3-II in cells subject to starvation-induced autophagy[11] and increased survival in deoxyrubicin treated cells that would normally undergo p53-mediated apoptosis.[5] We note that examination of medical histories in the reported subjects with *DRAM2*-associated retinal dystrophy provided no evidence of increased susceptibility to cancer.

Although *DRAM2* is transcribed ubiquitously (Figure S4),[6] in light of the finding that human *DRAM2* variants cause retinal dystrophy, we investigated the precise distribution of the normal protein in the mouse retina. Serial sections were taken from mouse eyes at postnatal day 30 and were stained with a goat polyclonal antiserum against DRAM2 (Figure 4). Confocal immunofluorescence microscopy showed that DRAM2 localized to the inner segment of the photoreceptor layer and the apical surface of the retinal pigment epithelium (RPE), which are located at the basal and distal ends of the outer segment respectively. This coincides with the primary pathology observed on pre-symptomatic OCT analysis in which the photoreceptor layer appeared specifically affected.

This localization is consistent with a role for DRAM2 in photoreceptor autophagy. Photoreceptor outer segments are in a constant state of renewal by ciliogenesis in response to light-induced damage. Recent studies have suggested that there is interplay between ciliogenesis and autophagy. In one study it was shown that disruption of ciliogenesis partially inhibited autophagy, while blocking autophagy enhanced primary cilia growth and cilia-associated signaling during normal nutritional conditions. The authors therefore proposed that basal autophagy regulated ciliary growth through the degradation of proteins required for intraflagellar transport.[12] In another study, the protein OFD1 (oral facial digital syndrome 1), which accumulated

at centriolar satellites located close to the base of the cilium, was rapidly degraded by serum starvation-induced autophagy. This led to ciliary growth, suggesting that OFD1 normally inhibited ciliogenesis.[13]

A high level of autophagy is also expected to take place in the RPE. These cells have a key role in processing shed photoreceptor outer segment discs and consequently, in removing toxic metabolites and recycling phototransduction components. This process which involves RPE phagocytosis causes up to 10% photoreceptor volume loss each day and is entrained to the circadian rhythm.[14,15] Indeed there is increasing interest in the role of autophagy in preserving photoreceptor function in connection with the circadian cycle,[16] the aging process[17] and retinal disease pathology.[18] It is therefore likely that the absence of DRAM2 in the retina reduces the efficiency of autophagy in recycling cell components, which in turn reduces photoreceptor renewal, leading to the thin photoreceptor layer observed on OCT which is the first presenting feature in pre-symptomatic patients.

To summarize, we have shown that biallelic missense, nonsense and frameshift variants in *DRAM2* cause retinal dystrophy with early macular cone photoreceptor involvement. The clinical features and course of retinal degeneration were highly similar among affected individuals from the five reported families. Our findings suggest that DRAM2 is essential for photoreceptor survival and further studies are expected to provide important insights into its precise role in the retina.

Acknowledgements

We would like to thank the patients and their families who participated in this study. We thank our colleagues at University College London, UK for kindly contributing to the UCL-exomes control panel. Additional members of the UK Inherited Retinal Disease Consortium include Graeme Black, Georgina Hall, Stuart Ingram, Rachel Gillespie, Simon Ramsden, Forbes Manson (Manchester Academic Health Science Centre, University of Manchester), Alison Hardcastle, Michel Michaelides, Michael Cheetham, Gavin Arno, Niclas Thomas, Shomi Bhattacharya, Tony Moore (UCL Institute of Ophthalmology and Moorfields Eye Hospital), Andrea Nemeth, Susan Downes, Stefano Lise (Division of Clinical Neurology, University of Oxford) and Emma Lord (Section of Ophthalmology and Neuroscience, University of Leeds). This

work was supported by grants from NERC (Yorkshire branch), Macular Society UK (www.maculardisease.org), the UK National Institute for Health Research (Biomedical Research Centre, Moorfields Eye Hospital and Institute of Ophthalmology), RP Fighting Blindness and Fight For Sight (RP Genome Project GR586), the Belspo IAP project P7/43, the Belgium Medical Genomics Initiative (BeMGI), the Ghent University Special Research Fund (BOF15/GOA/011) and the Funds for Research in Ophthalmology (FRO). CAJ and CFI were supported by a grant from the Jules Thorn Charitable Trust. MEE is funded by an Egyptian Government Scholarship and KVS is a doctoral fellow from the Institute for Innovation by Science and Technology (IWT). EDB and BPL are senior clinical investigators of the Research Foundation Flanders (FWO).

Web Resources

The URLs for data presented herein are as follows:

AgileMultiIdeogram, http://dna.leeds.ac.uk/agile/AgileMultiIdeogram/
ANNOVAR, http://www.openbioinformatics.org/annovar/
CADD, http://cadd.gs.washington.edu/
ClustalW, http://www.ebi.ac.uk/clustalw2/
dbSNP, http://www.ncbi.nlm.nih.gov/SNP/
ExAC browser, http://exac.broadinstitute.org/
Galaxy, https://usegalaxy.org
GATK, http://www.broadinstitute.org/gsa/wiki/index.php/The_Genome_Analysis_Toolkit
IGV (Interactive Genomics Viewer), http://www.broadinstitute.org/software/igv/
Mutation Taster, http://www.mutationtaster.org/
MutPred, http://mutpred.mutdb.org/
NHLBI Exome Sequencing Project Exome Variant Server (EVS), http://evs.gs.washington.edu/
Online Mendelian Inheritance in Man (OMIM), http://www.omim.org/
Picard, http://picard.sourceforge.net/
PolyPhen2, http://genetics.bwh.harvard.edu/pph2/
Primer3, http://frodo.wi.mit.edu/cgi-bin/primer3/
PROVEAN, http://provean.jcvi.org/
RetNet, https://sph.uth.edu/retnet/home.htm
SIFT, http://sift.jcvi.org/
Superlink, http://cbl-hap.cs.technion.ac.il/superlink-snp/

References

1. Wright, A.F., Chakarova, C.F., Abd El-Aziz, M.M., Bhattacharya, S.S. (2010). Photoreceptor degeneration: genetic and mechanistic dissection of a complex trait. Nat. Rev. Genet. 11, 273–284.

2. Silberstein, M., Tzemach, A., Dovgolevsky, N., Fishelson, M., Schuster, A., Geiger, D. (2006). Online system for faster multipoint linkage analysis via parallel execution on thousands of personal computers. Am. J. Hum. Genet. 78, 922-935.

3. Sergouniotis, P.I., Chakarova, C., Murphy C., Becker M., Lenassi E., Arno G., Lek M., MacArthur D.G., UCL-Exomes Consortium, Bhattacharya S.S., et al. (2014). Biallelic variants in TTLL5, encoding a tubulin glutamylase, cause retinal dystrophy. Am. J. Hum. Genet. 94, 5, 760-769.

4. Pearson, R.D. (2011). Bias due to selection of rare variants using frequency in controls. Nat. Genet. 43, 392–393, author reply 394–395.

5. Park, S.M., Kim, K., Lee, E.J., Kim, B.K., Lee, T.J. Seo, T., Jang, I.S., Lee, S.H., Kim, S., Lee, J.H., et al. (2009). Reduced expression of DRAM2/TMEM77 in tumor cells interferes with cell death. Biochem. Biophys. Res. Commun. 4, 1340-1344.

6. O'Prey, J., Skommer, J., Wilkinson, S., Ryan, K.M. (2009). Analysis of DRAM-related proteins reveals evolutionarily conserved and divergent roles in the control of autophagy. Cell Cycle 8, 2260– 2265.

7. Levine, B., Klionsky, D.J. (2004). Development by self-digestion: molecular mechanisms and biological functions of autophagy. Dev. Cell 6, 463-477.

8. Yoshimori, T. (2004). Autophagy: a regulated bulk degradation process inside cells. Biochem. Biophys. Res. Commun. 313, 453-458.

9. Kroemer, G., Jäättelä, M. (2005). Lysosomes and autophagy in cell death control. Nat. Rev. Cancer 5, 886-897.

10. Yuan, J., Lipinski, M., Degterev, A. (2003). Diversity in the mechanisms of neuronal cell death. Neuron 40, 401-413.

11. Yoon, J.H., Her, S., Kim, M., Jang, I.S., Park, J. (2012). The expression of damage-regulated autophagy modulator 2 (DRAM2) contributes to autophagy induction. Mol. Biol. Rep. 39, 1087-1093.

12. Pampliega, O., Orhon, I., Patel, B., Sridhar, S., Díaz-Carretero, A., Beau, I., Codogno, P., Satir, B.H., Satir, P., Cuervo, A.M. (2013) Functional interaction between autophagy and ciliogenesis. Nature 502, 194-200.

13. Tang, Z., Lin, M.G., Stowe, T.R., Chen, S., Zhu, M., Stearns, T., Franco, B., Zhong, Q. (2013) Autophagy promotes primary ciliogenesis by removing OFD1 from centriolar satellites. Nature 502, 254-257.

14. Young, R.W., Bok, D. (1969). Participation of the retinal pigment epithelium in the rod outer segment renewal process. J. Cell Biol. 42, 392–403.

15. Nguyen-Legros, J., Hicks D. (2000) Renewal of photoreceptor outer segments and their phagocytosis by the retinal pigment epithelium. Int. Rev. Cytol. 196, 245-313.

16. Yao, J., Jia, L., Shelby, S.J., Ganios, A.M., Feathers, K., Thompson, D.A., Zacks, D.N. (2014). Circadian and noncircadian modulation of autophagy in photoreceptors and retinal pigment epithelium. Invest. Ophthalmol. Vis. Sci. 55, 3237-3246.

17. Rodríguez-Muela, N., Koga, H., García-Ledo, L., de la Villa, P., de la Rosa, E.J., Cuervo, A.M., Boya, P. (2013). Balance between autophagic pathways preserves retinal homeostasis. Aging Cell 12, 478-488.

18. Métrailler, S., Schorderet, D.F., Cottet, S. (2012). Early apoptosis of rod photoreceptors in Rpe65(-/-) mice is associated with the upregulated expression of lysosomal-mediated autophagic genes. Exp. Eye Res. 96, 70-81.

Figure 1. Clinical features of individuals from family ES1 with retinal dystrophy and early maculopathy caused by recessive *DRAM2* mutations.

Colour fundus photograph (A), fundus autofluorescence (C), infra-red reflectance (E) and OCT (F) images from the right eye of case IV.9 at 25 years. Corresponding images from an unaffected individual are provided for comparison (B, D, G and H). Macular atrophy with white dots at its temporal edge are observed on fundus photography. On autofluorescence imaging, there is a central area of reduced autofluorescence surrounded by a hyperautofluorescent ring. On OCT imaging, there is significant thinning in the foveal region consistent with photoreceptor loss. A composite colour photograph from the left eye of case III.1, at the age of 48, is also shown (I). This reveals macular atrophy, mid-peripheral bone-spicule pigmentation and attenuated retinal vessels. On the infra-red reflectance images, the horizontal green lines indicate the position and direction of the corresponding OCT scan. The scale bars represent 200μm.

Figure 2. Pedigrees of families/cases reported in this study and *DRAM2* mutation segregation data.

Affected individuals are shaded black. The maternal grandmother of individual gc17004 has age-related macular degeneration in her 90s (shaded grey). The genotypes for all tested family members are shown below each individual, with M representing the mutant allele and + representing the wild-type allele.

Figure 3. Variants in *DRAM2* cause retinal dystrophy.

(A) Schematic representation of the *DRAM2* genomic structure and major transcript (NM_178454.4) showing the location and sequence traces of the seven disease-causing variants identified in this study. (B) Schematic diagram of the DRAM2 protein showing the location of the affected amino-acids within the protein domains.

Figure 4. Localization of DRAM2 to the photoreceptor inner segments and retina pigment epithelium.

Radial 6μm cryosections of mature mouse retina (P30) were labeled with anti-DRAM2 (M-12, Santa Cruz Biotechnology) and anti-Rhodopsin (Sigma-Aldrich) followed by the secondary antibody Alexa Fluor 568-conjugated donkey anti-goat immunoglobulin (red) (Molecular Probes Incorporation) and Alexa Fluor 488-

conjugated chicken anti-rabbit immunoglobulin (green) (Molecular Probes Incorporation) respectively, and the nuclei counterstained with DAPI (Vector Laboratories). An independent section stained with both secondary antibodies only and another with peptide (Santa Cruz Biotechnology, sc-241077-P)-competition against the DRAM2 primary antibody served as negative controls in the experiment. Immunofluorescence was analyzed with an Eclipse TE2000-E inverted confocal microscope (Nikon Instruments) and shows localisation of DRAM2 to the inner segment of the photoreceptor layer (PIS) and the retinal pigment epithelium (RPE). Rhodopsin localises to the outer segment of the photoreceptor layer (POS). The other layers are the outer nuclear layer (ONL), outer plexiform layer (OPL), inner nuclear layer (INL), inner plexiform layer (IPL) and the ganglion cell layer (GCL). Scale bar represents 50μm.

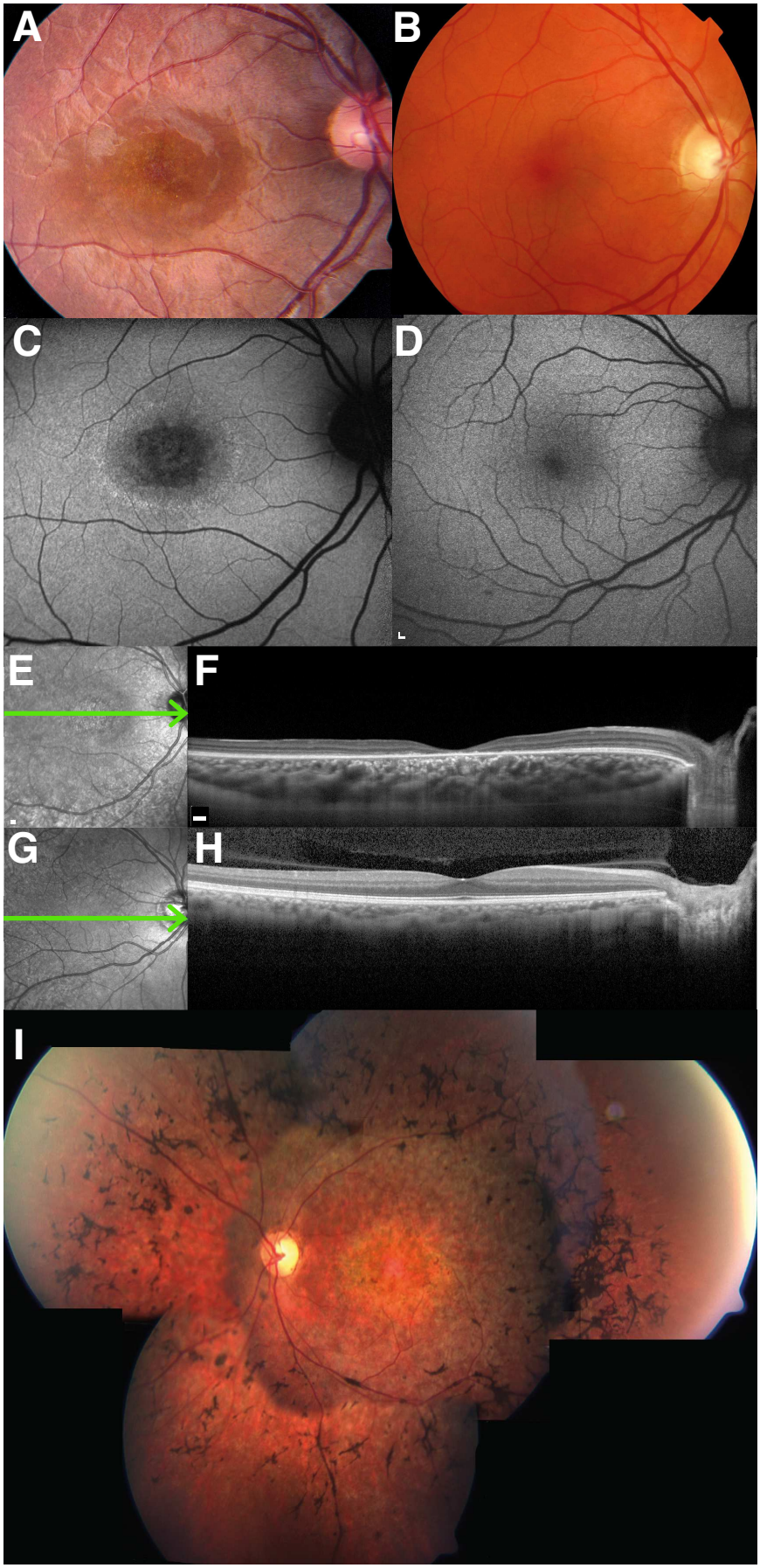
A
B
C
D
E
F
G
H
I

Family ES1
c.140delG (p.Gly47Valfs*3)

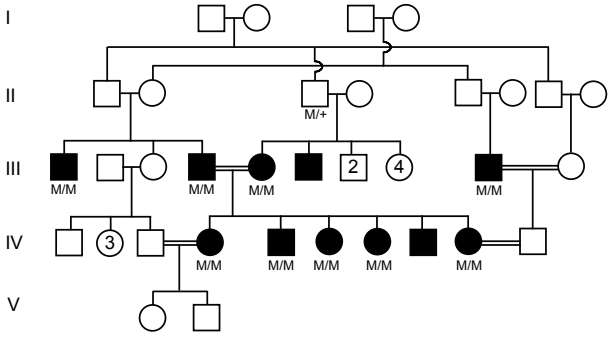

Case 1325
M1= c.131G>A (p.Ser44Asn)
M2 = c.494G>A (p.Trp165*)

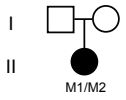

Family gc4728
c.362A>T (p.His121Leu)

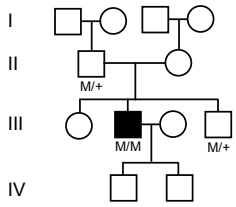

Family gc17004
M1 = c.79T>C (p.Tyr27His)
M2 = c.217_225del (p.Val73_Tyr75del)

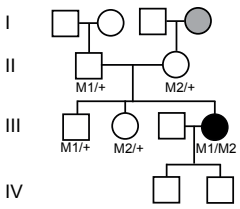

Family BL1
c.64_66del (p.Ala22del)

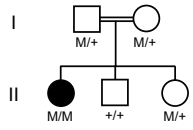

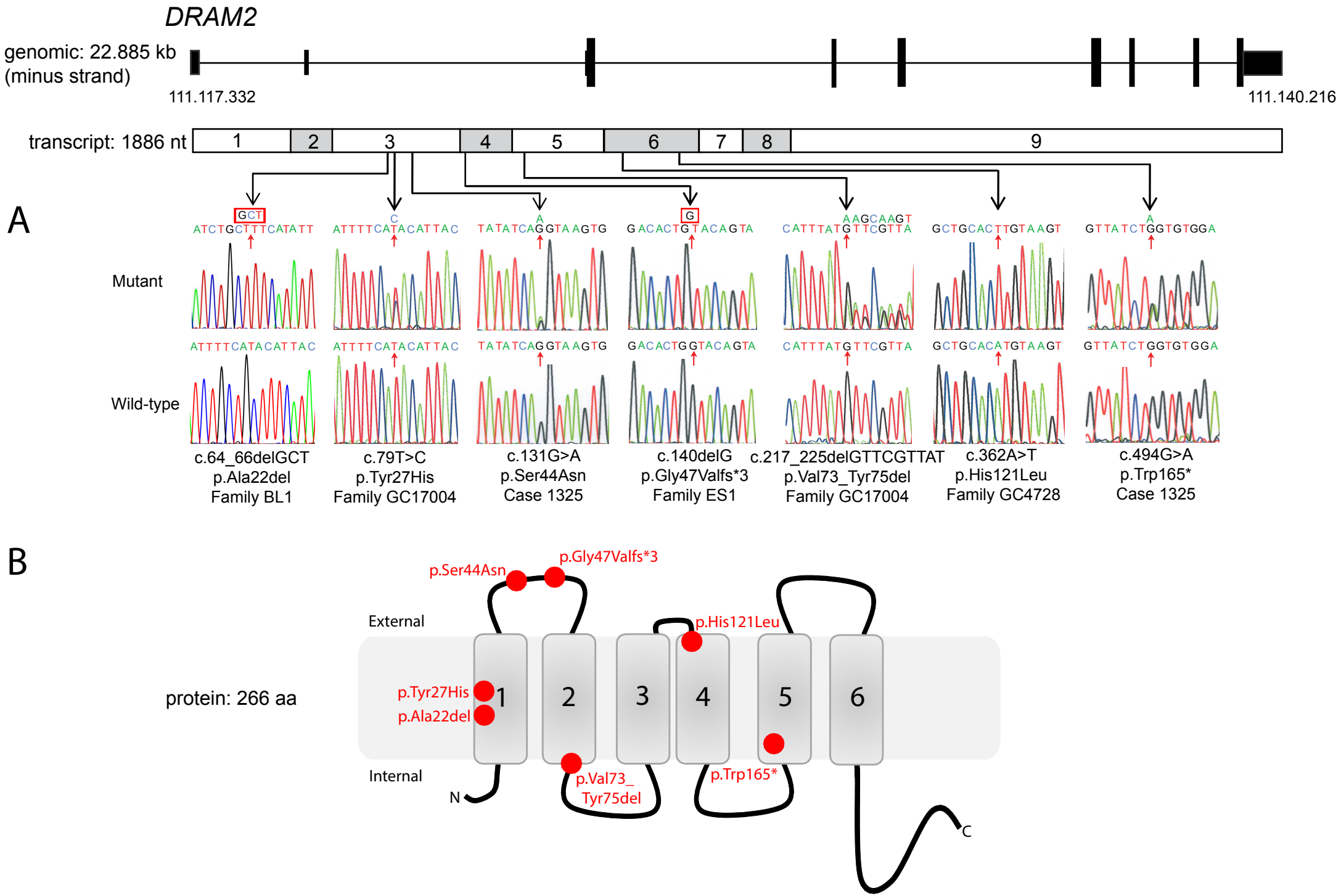
DRAM2
genomic: 22.885 kb
(minus strand)
111.117.332
111.140.216
transcript: 1886 nt
1
2
3
4
5
6
7
8
9
A
Mutant
Wild-type
c.64_66delGCT
p.Ala22del
Family BL1
c.79T>C
p.Tyr27His
Family GC17004
c.131G>A
p.Ser44Asn
Case 1325
c.140delG
p.Gly47Valfs*3
Family ES1
c.217_225delGTTCGTTAT
p.Val73_Tyr75del
Family GC17004
c.362A>T
p.His121Leu
Family GC4728
c.494G>A
p.Trp165*
Case 1325
B
protein: 266 aa
External
Internal
N
C
p.Ser44Asn
p.Gly47Valfs*3
p.His121Leu
p.Tyr27His
p.Ala22del
p.Val73_
Tyr75del
p.Trp165*

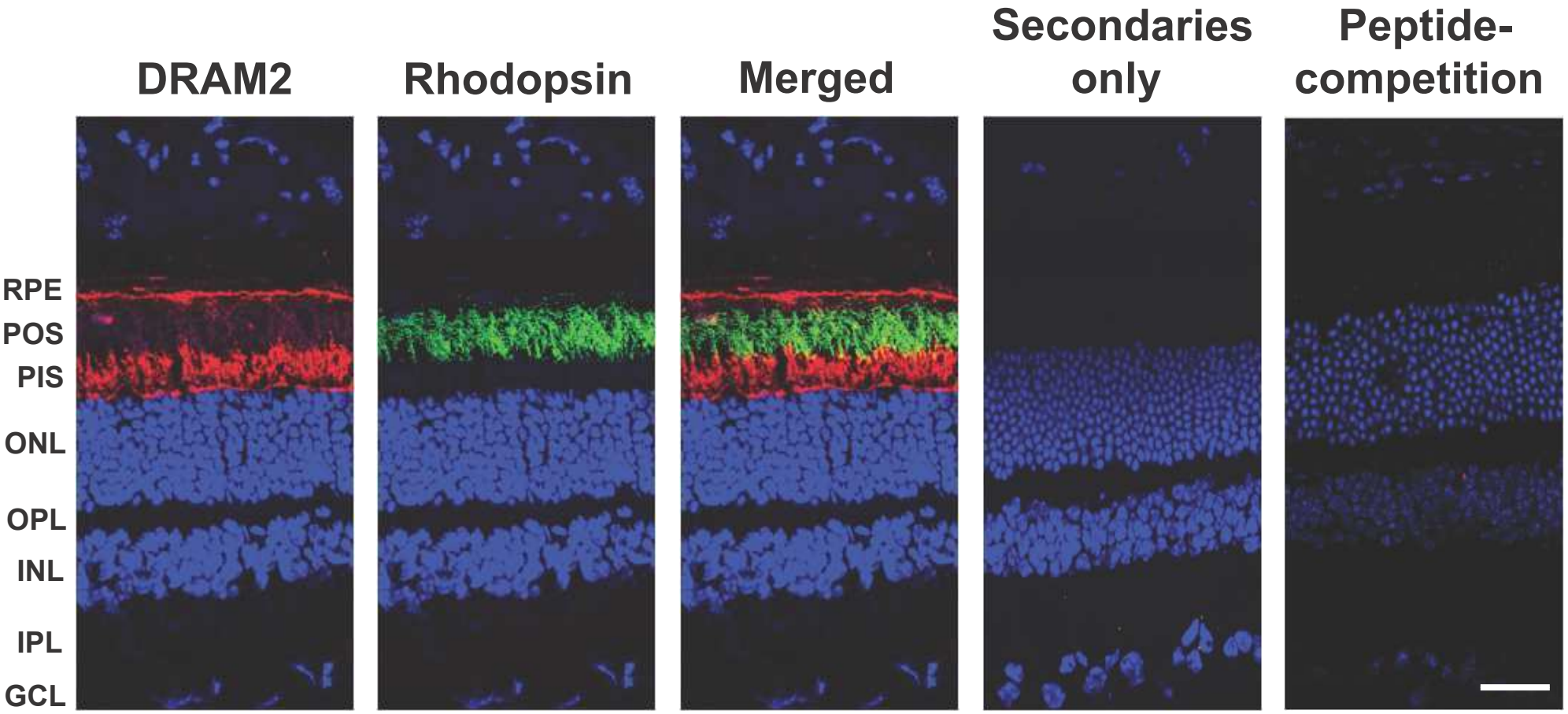
DRAM2
Rhodopsin
Merged
Secondaries only
Peptide-competition
RPE
POS
PIS
ONL
OPL
INL
IPL
GCL

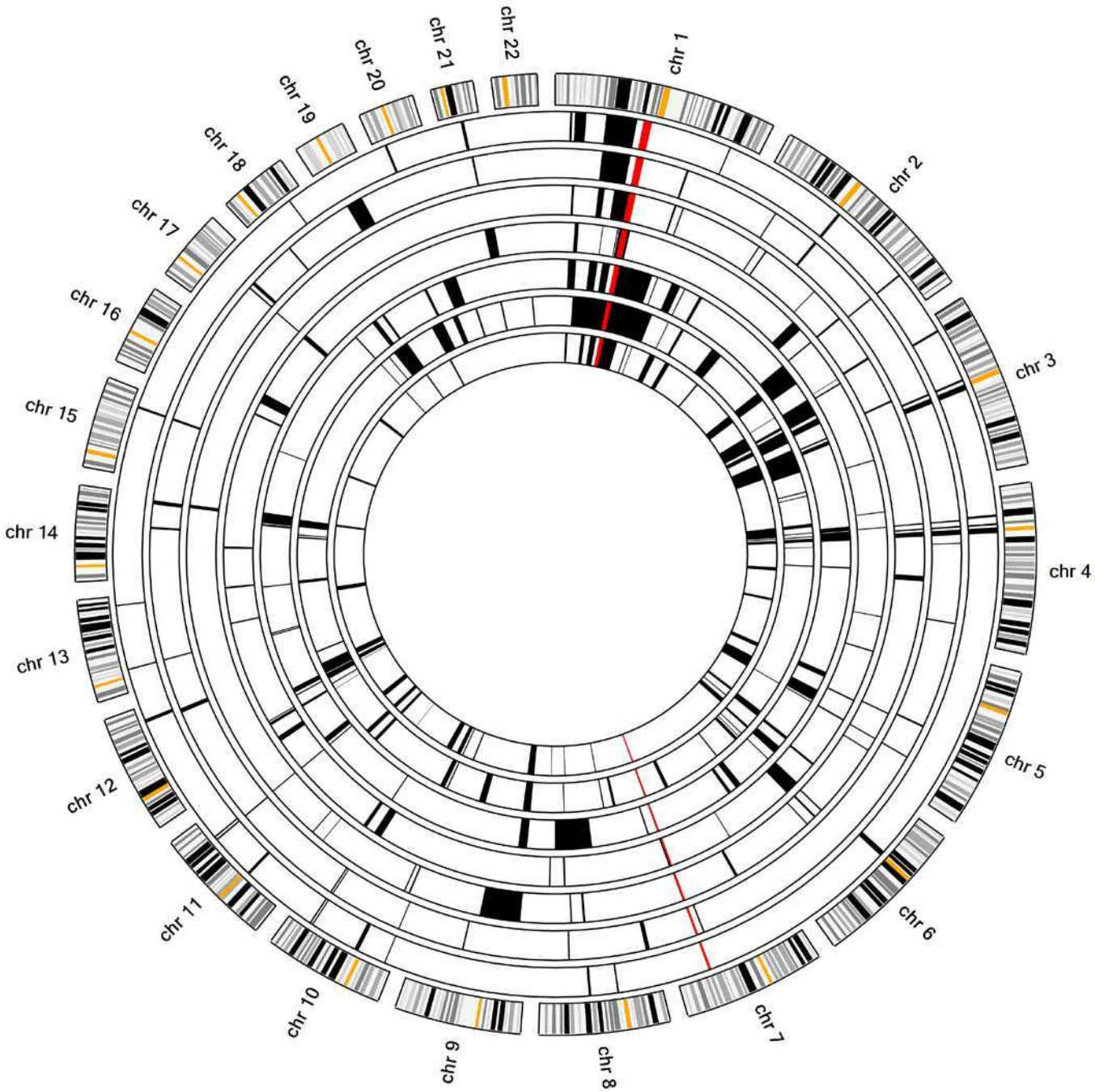

Figure S1. Autozygosity mapping in family ES1. The schematic results generated by AgileMultiIdeogram software are shown (http://dna.leeds.ac.uk/agile/AgileMultiIdeogram/). The figure displays the locations of homozygous regions identified from SNP genotyping data from multiple individuals against a circular ideogram of chromosomes 1–22. Data for individuals III.1, III.4, III.5, III.13, IV.6, IV.8 and IV.11 are shown. The homozygous regions in each family member are shown in black. The common autozygous regions identified in all affected family members are highlighted in red. A large region spanning over 10Mb was identified on chromosome 1 (Chr1:106188422-116250460 hg38) and a smaller region spanning >3Mb on chromosome 7 (Chr7:117088307-119982844 hg38).

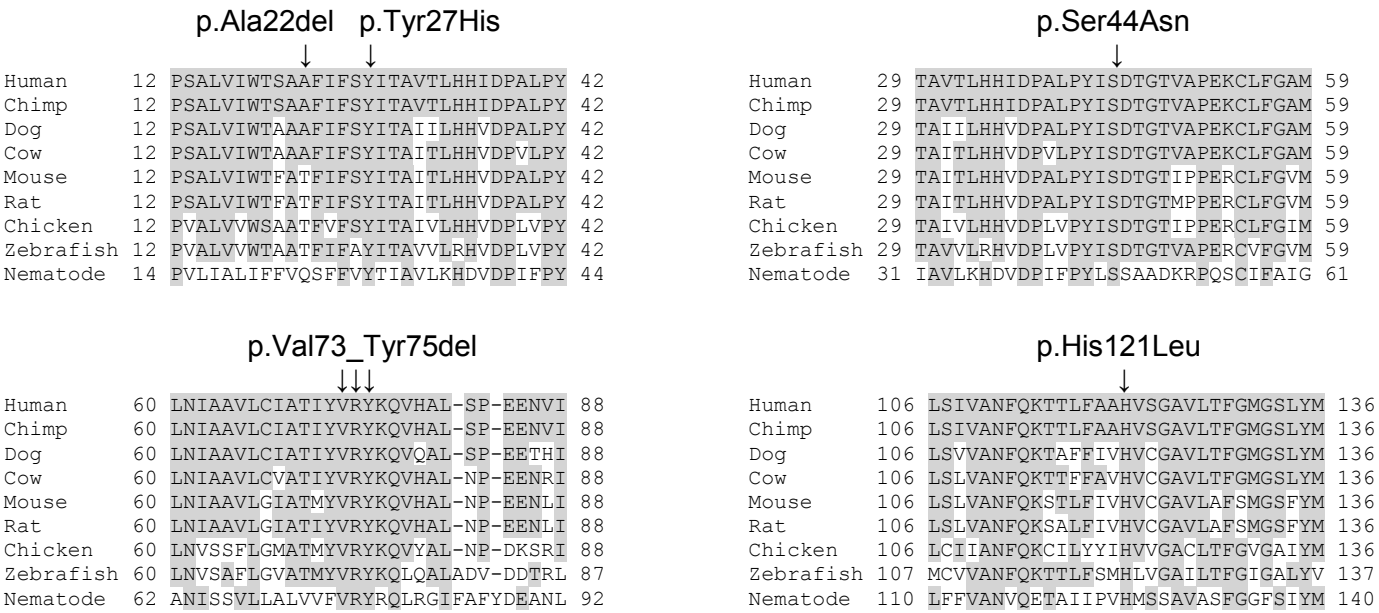

Figure S2. Protein sequence alignment of human DRAM2 with orthologues. Multiple protein alignments were calculated using HomoloGene (http://www.ncbi.nlm.nih.gov/homologene) [Edgar, R.C. (2004) Nucleic Acids Res. 32, 1792-7]. Thirty amino acid residues surrounding each mutation are shown. Conserved amino acid residues are shaded. The positions of the missense mutations p.Tyr27His, p.Ser44Asn and p.His121Leu are indicated along with the in-frame deletions p.Ala22del and p.Val73_Tyr75del. Accession numbers: Human NP_848549.3; Chimpanzee XP_001162049.1; Dog XP_005621845.1; Cow NP_001070464.1; Mouse NP_080289.1; Rat NP_001020189.1; Chicken XP_003642762.1; Zebrafish NP_001002135.1; Nematode NP_510541.1.

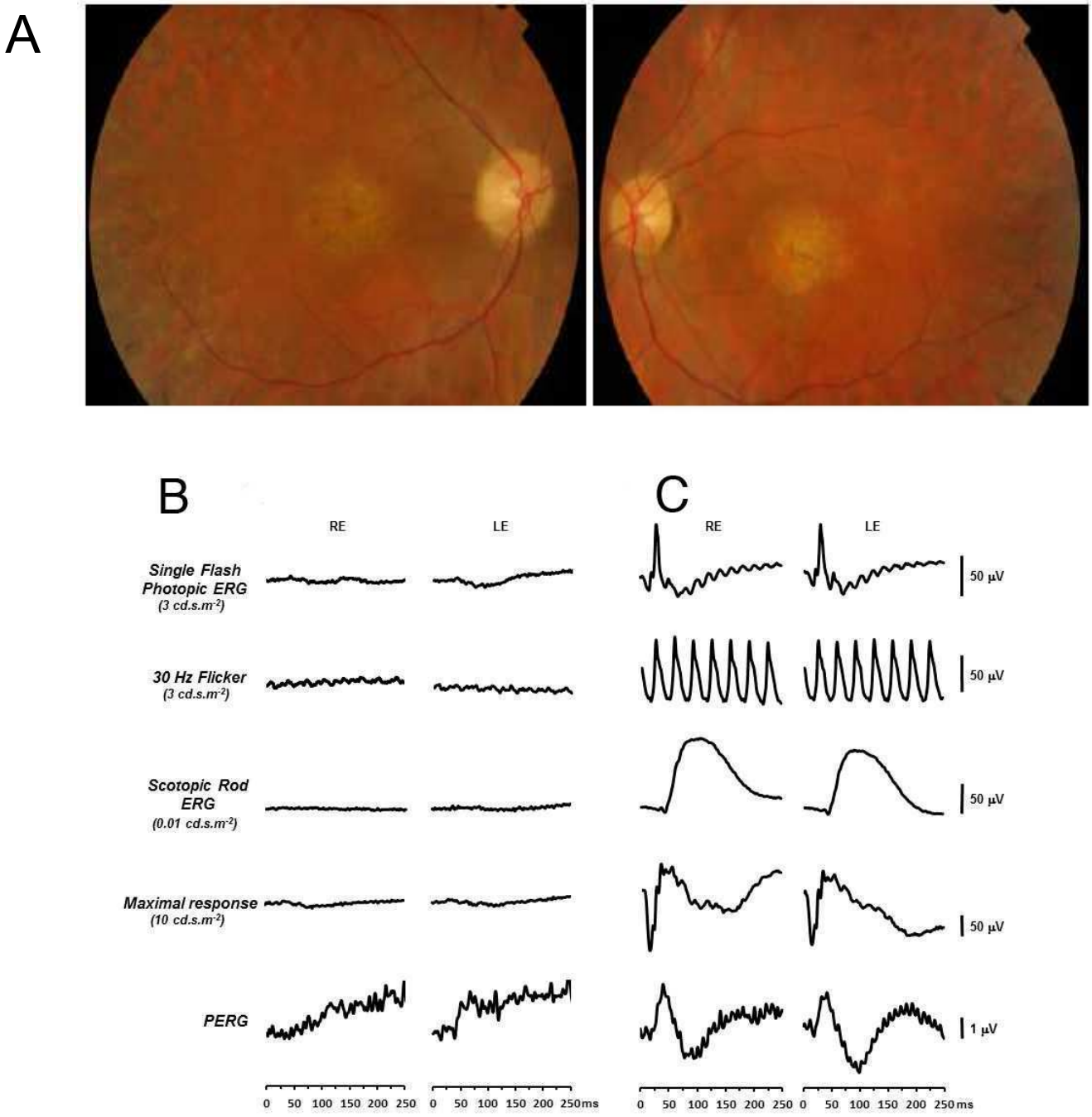

Figure S3. Clinical features of Case 1325 with a diagnosis of retinal dystrophy and early maculopathy. Fundus photographs of the right and left eyes at 35 years of age (A) shows central macular atrophy with grey dots in the temporal macula with intra-retinal pigment migration. Flash and pattern electroretinography (ERG and PERG) of the case (at 46 years of age) (B) and a normal control individual (C) were recorded to ISCEV standard protocols for the right (RE) and left (LE) eyes. Light-adapted single flash photopic ERG, 30Hz flicker (cone-isolating) ERG, dark-adapted scotopic rod ERG and PERG traces were all severely attenuated or absent compared to the normal control values suggesting a generalised rod-cone dysfunction. The attenuated PERGs indicate that the central macular region is affected by this condition.

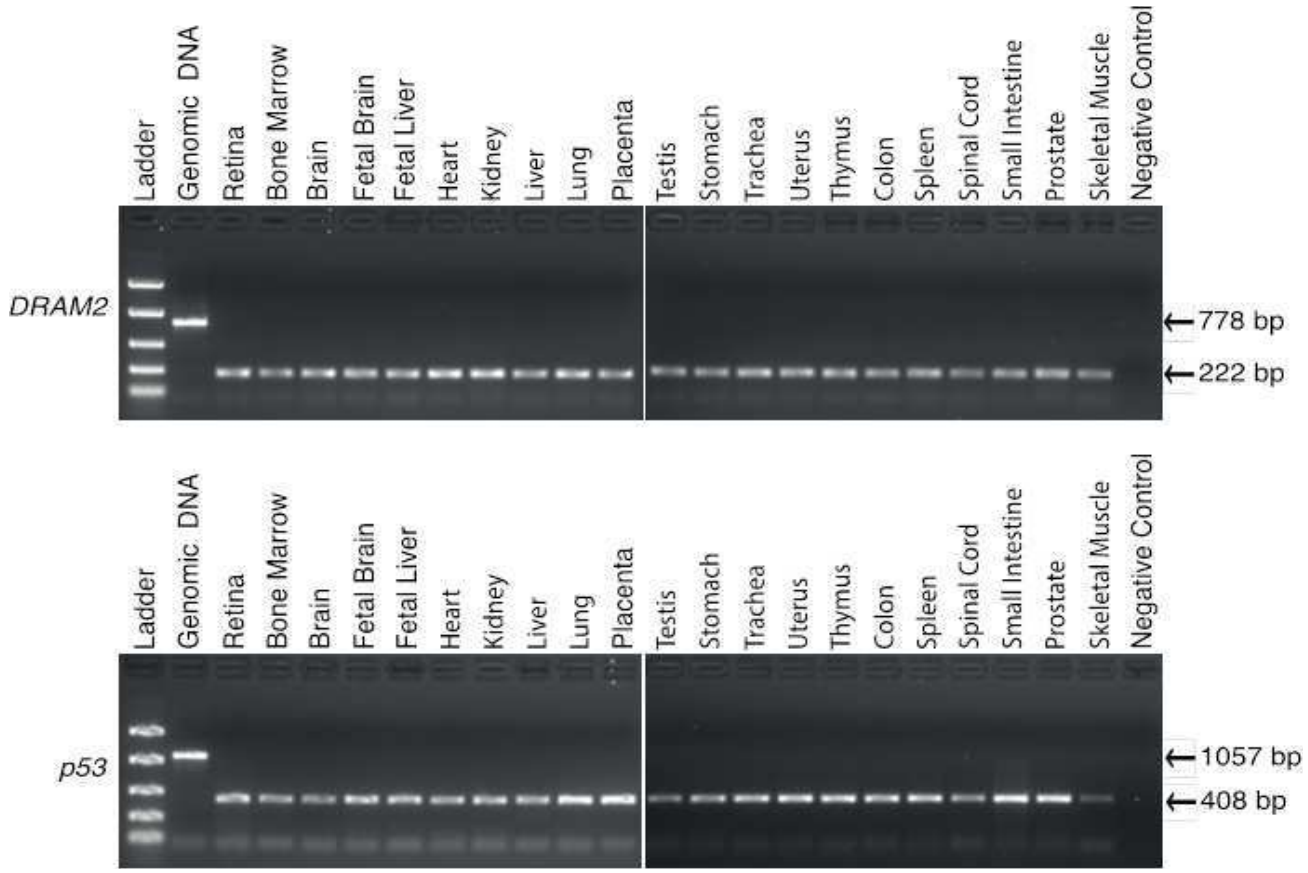

Figure S4. *DRAM2* mRNA is ubiquitously expressed in all human tissues analysed. Human adult and fetal tissue total RNA was purchased from Clontech and converted to cDNA using standard protocols. The retina cDNA was purchased from Clontech. A 222-bp fragment of *DRAM2* spanning intron 6 was amplified from the cDNAs using primers DRAM2_RT_F 5'-GGAGCTGTGCTTACCTTTGG-3' and DRAM2_RT_R 5'-GGGGTTCCAATGGAGTTTCT-3' (genomic PCR size = 778 bp). P53 control primers used were P53 RT-F 5'-GTACTCCCCTGCCCTCAACA-3' and P53 RT-R 5'-CTGGAGTCTTCCAGTGTGAT-3' (cDNA product size = 408 bp, genomic PCR size = 1057 bp).

Table S1. Summary of variants after filtering whole exome sequencing output from patient IV:6 in Family ES1.

Chromosome	Gene	Effect	cDNA change	Protein change
1	*HMGB4*	Missense	NM_145205:exon2:c.C345A	p.N115K
1	*GJB5*	Missense	NM_005268:exon2:c.C166T	p.R56C
1	*DRAM2*	Frameshift deletion	NM_178454:exon4:c.140delG	p.G47fs
1	*LY9*	Missense	NM_001261456:exon5:c.A1238G	p.N413S
2	*NEB*	Missense	NM_004543:exon131:c.T17909C	p.I5970T
2	*LY75*	Missense	NM_001198759:exon12:c.C1960T	p.L654F
3	*LOC401052*	Missense	NM_001008737:exon4:c.A287C	p.H96P
5	*SPEF2*	Missense	NM_024867:exon5:c.A601G	p.R201G
5	*BRD8*	Missense	NM_139199:exon9:c.C671T	p.S224F
6	*CD109*	Missense	NM_001159588:exon4:c.A385G	p.I129V
6	*ZNF292*	Missense	NM_015021:exon8:c.A8132G	p.D2711G
7	*FZD1*	Missense	NM_003505:exon1:c.G1578T	p.K526N
10	*GPRIN2*	Missense	NM_014696:exon3:c.A724G	p.R242G
10	*ADAMTS14*	Missense	NM_080722:exon16:c.C2363T	p.A788V
10	*RRP12*	Missense	NM_001145114:exon24:c.G2847C	p.K949N
10	*GBF1*	Missense	NM_001199378:exon3:c.C112A	p.P38T
11	*OR51V1*	Missense	NM_001004760:exon1:c.G286C	p.G96R
11	*OR52H1*	Missense	NM_001005289:exon1:c.G3T	p.M1I
12	*PLEKHG6*	Nonsense	NM_001144857:exon9:c.C1023G	p.Y341X
12	*TAPBPL*	Missense	NM_018009:exon1:c.G49A	p.G17R
12	*NUAK1*	Missense	NM_014840:exon1:c.A32G	p.D11G
16	*SOCS1*	Missense	NM_003745:exon2:c.C116G	p.P39R
17	*CD300C*	Missense	NM_006678:exon2:c.G103C	p.V35L
19	*PLIN4*	Missense	NM_001080400:exon3:c.A2200G	p.I734V
19	*OR10H3*	Missense	NM_013938:exon1:c.G293T	p.C98F
19	*OR10H4*	Missense	NM_001004465:exon1:c.G293T	p.C98F
19	*ZNF773*	Missense	NM_198542:exon4:c.C290A	p.A97E
21	*USP16*	Missense	NM_001001992:exon14:c.A1829G	p.E610G
X	*SHROOM2*	Missense	NM_001649:exon4:c.C2725G	p.Q909E
X	*APEX2*	Missense	NM_001271748:exon5:c.G509A	p.R170H
X	*CYLC1*	Missense	NM_001271680:exon1:c.G14C	p.R5T
X	*TCEAL5*	Missense	NM_001012979:exon3:c.C246A	p.D82E
X	*MAGEA10*	Missense	NM_021048:exon4:c.A1014C	p.E338D

For whole exome sequencing, exon capture was performed using the SureSelectXT Human All Exon V4 target enrichment reagent (Agilent) and paired-end sequencing was completed on a HiSeq2000 system (Illumina). The raw sequence data files were processed on the Galaxy platform and aligned to the human reference genome sequence (hg19/GRCh37) using Bowtie2. The alignment was processed in BAM format with Picard and the Genome Analysis Toolkit to correct alignments around insertions-deletions, and to identify and remove duplicates and sequencing reads with quality scores less than 20. The Unified Genotyper reported variants in the VCF format which were annotated using ANNOVAR. For filtering, we excluded variants (i) with a read depth of less than 10, (ii) that were outside the exon and flanking two base-pair splice donor and acceptor sites, (iii) that were synonymous and (iv) with a minor allele frequency (MAF) >1% in the NHLBI Exome Sequencing Project Exome Variant Server (EVS; release version v.0.0.30) or the 1000 Genomes Project.

Table S2. *DRAM2* primers for PCR/sequencing.

Exon	Forward primer (5'-3')	Reverse primer (5'-3')	Size (bp)
3	GAAACAGCTTGGGGTGGTAA	CACAAAGAAAAAGCCAAATTCA	414
4	GGTGAAGTAGGCAGATATTTGTGA	TTCCCATAAGTCCGCATTTC	442
5	TCCAGCCTGTGCAACATAGA	GAATGCTTCAGGTTTCCCTTT	429
6	TTGTAGAATTGGCCGAGCTT	AAAGGCTTCTTATACTGCACCAA	400
7	ACCCTCTGAGCAGCACATTT	GGTGACAGGAGAATATGGAAGG	442
8	GCCTGGTAAGTCAAGGGTTG	TAGCCCCATTTTCAAGGCTA	447
9	TGAGAAGCTTGGTTTTTCCAG	TGGCTTCTTTCATGTTTCCTG	450

Table S3. Summary of bioinformatics analyses undertaken to predict the pathogenic nature of the *DRAM2* missense variants and in-frame deletions.

Variant	PolyPhen2	MutationTaster	SIFT	Blosum62*	CADD**	PROVEAN	MutPred
p.Ala22del	N/A	Disease causing (prediction probability 0.9999)	N/A	N/A	Scaled C-score = 18.84	Deleterious (score -7.523)	N/A
p.Tyr27His	Probably damaging (score 1.000)	Disease causing (prediction probability 0.9999)	Damaging (score 0.000)	Score +2	Scaled C-score = 22.8	Deleterious (score -4.029)	Deleterious mutation (prediction probability 0.742)
p.Ser44Asn	Probably damaging (score 0.999)	Disease causing (prediction probability 0.9999)	Damaging (score 0.000)	Score +1	Scaled C-score = 22.5	Deleterious (score -2.650)	Deleterious mutation (prediction probability 0.879)
p.Val73_Tyr75del	N/A	Polymorphism (prediction probability 0.9867)	N/A	N/A	Scaled C-score = 17.47	Deleterious (score -23.371)	N/A
p.His121Leu	Probably damaging (score 0.999)	Disease causing (prediction probability 0.9999)	Damaging (score 0.000)	Score -3	Scaled C-score = 24.6	Deleterious (score -10.605)	Deleterious mutation (prediction probability 0.906)

URLs: PolyPhen2, http://genetics.bwh.harvard.edu/pph2/ [Adzhubei, I.A. et al. (2010). Nat. Methods 7, 248-9]; Mutationtaster, http://www.mutationtaster.org/ [Schwarz, J.M. et al. (2010). Nat. Methods 7, 575-6]; SIFT, http://sift.jcvi.org/ [Ng, P.C. et al. (2003). Nucleic Acids Res. 31, 3812-4]; Blosum62 [Henikoff, S. et al. (1993). Proteins 17, 49-61]; CADD, http://cadd.gs.washington.edu [Kircher, M. et al. (2014). Nat. Genet. 46:310-5]; PROVEAN, http://provean.jcvi.org/ [Choi, Y. et al. (2012). PLoS ONE 7, e46688]; MutPred, http://mutpred.mutdb.org/ [Li, B. et al. (2009). Bioinformatics 25, 2744-50]. *Blosum62 scores range from +3 to -3 and negative scores are more likely to be damaging substitutions. **CADD scores are reported as scaled C-scores and values ≥ 20 and ≥ 10 respectively represent the 1% and 10% most deleterious changes predicted in the human genome.

Table S4. **Top five most significant autosomal genes: the count of rare non-synonymous variants in likely homozygous or compound heterozygous state was compared between probands with retinal dystrophy and internal controls.**

	Chromosome	Cases* (n_{max}=18)		Controls** (n_{max}=1,917)		Binomial p value
		Likely compound heterozygotes	Likely homozygotes	Likely compound heterozygotes	Likely homozygotes	
DRAM2	1	1	1	0	0	0.0001
SELP	1	1	1	5	1	0.0026
ADAP2	17	0	1	0	0	0.0095
GOLGA1	9	0	1	0	0	0.0095
CCDC134	22	0	1	0	0	0.0096

*Case group: 18 probands with (i) a retinal dystrophy with early cone photoreceptor involvement (macular dystrophy or cone rod dystrophy), (ii) absence of fundoscopic and fundus autofluorescence imaging features suggestive of *ABCA4*-retinopathy and (iii) an unknown molecular diagnosis after inspection of exome sequencing data for causal variants in known retinal dystrophy genes. The exomes from all cases were prepared using the Agilent SureSelectXT Human All Exon V5 capture and an Illumina HiSeq2000 sequencer.

**UCL-exomes control samples: 1,917 unrelated individuals, predominantly of European origin, with no diagnosis of retinal disease. Exome sequencing data from controls was analyzed using the same sequence variant-calling strategy as the cases. Variants with a read depth <7 were ignored.

We considered a case, or a control, as a "recessive disease candidate" if it harboured ≥2 potentially functional (presumed loss-of-function, non-synonymous or splice site altering) rare variants in the heterozygous state ("likely compound heterozygotes") or ≥1 potentially functional, rare variant in the homozygous state ("likely homozygotes"). As "rare" we defined changes that: (i) had a minor allele frequency of <0.5% in the EVS dataset and (ii) had <2 occurrences in 500 additional UCL-exomes control samples; the latter were randomly sampled and not included directly in the case-control analysis. The BAM files were inspected using the Integrative Genomics Viewer (IGV) and obvious artefacts were removed. This IGV check also excluded pairs of genetic variants located on the same haplotype, when evidenced by the presence of both variants on the same short sequencing reads.

For each gene, the number of 'recessive disease candidates' was determined in the case and control groups. To remove false homozygous calls that might result from low sequencing depth, we excluded variants with a read depth of 6 or less. Autosomal genes were then ranked based on a binomial p value test. This test computes the exact probability of seeing the observed number, or more, of 'recessive disease candidates' in cases under the assumption that the prevalence in cases was equal to that in controls, using the binomial distribution. This binomial test required a sample size estimate in cases and controls, which varied between genes owing to variable coverage. To estimate these two numbers for each gene, we listed all polymorphic coding positions within that gene and we computed the average of non-missing calls. This average was the number that was used in the binomial test.